

## EXPLORING THE INFLUENCE OF FEMUR BONE ANATOMICAL VARIABILITY ON CAM MORPHOLOGY

Dominic Bachmann<sup>1</sup>, Ted Yeung<sup>2</sup>, Thor Besier<sup>2</sup> & Wolfgang Potthast<sup>2</sup>

<sup>1</sup>Institute of Biomechanics and Orthopaedics, German Sport University Cologne, Cologne, Germany

<sup>2</sup>Auckland Bioengineering Institute, University of Auckland, Auckland, New Zealand

The purpose of this study was to identify potential femoral geometrical risk factors on cam morphology development and its implications for athletes. 382 segmentations from CT-scans were analysed. Cam morphology was defined by an average distance deviation (ADD) between a healthy fit onto the proximal femur and the segmented proximal femur at the anterolateral head-neck junction and categorized into four groups. Neck-shaft angle, femoral anteversion, neck length and femur length described the femur geometry. Neck-shaft angle demonstrated a significant effect on the ADD. Additionally, a novel method for automatically characterizing femur morphology was developed, offering potential applications in diagnosing cam deformities. The findings suggest that the neck-shaft angle may serve as a risk factor in the development of cam morphology.

**KEYWORDS:** cam, statistical shape model, femoroacetabular impingement.

**INTRODUCTION:** Cam morphology, characterized by asphericity of the femoral head-neck junction (Ito, Minka, Leuning, Werlen, & Ganz, 2001) poses a risk factor in the early development of osteoarthritis at the hip. Male adolescent athletes engaged in high impact sports are prone to developing a cam deformity during closure of the femoral epiphysis and are more likely to end a professional career early (Palmer, et al., 2018). Mechanically, a cam deformity narrows the space between the acetabulum and the femur leading to a premature impingement on soft tissue. Impingement causes symptoms such as groin pain and reduced internal rotation, known as femoroacetabular impingement syndrome (FAIS) (Palmer, et al., 2018). Diagnosis currently relies on clinical tests and radiographic measurements of the proximal femur, typically identified by an alpha-angle  $> 55^\circ$ , although this threshold is debated in the literature (Agricola, et al., 2014). However, radiographic measurements are derived from planar imaging despite cam morphology being three dimensional. Furthermore, existing imaging techniques only capture the proximal femur impeding the analysis of the overall femoral geometry and hence to better understand the relationship between femur geometry and cam morphology (Agricola, et al., 2014). Therefore, the aim of this study was to analyse potential cam deformities using a mean surface deviation from a 'healthy' reference statistical shape model (SSM) and examine the relationship between cam deformity and femur geometry. Our long-term aim is to provide a quantitative tool to diagnose and assess athletes with cam morphology.

**METHODS:** A proximal femur SSM trained on 20 healthy male proximal femurs with no cam morphology was used to predict a 'healthy' shape of 382 male proximal femur segmentations from CT scans of the Victorian Institute of Forensic Medicine (0.82 x 0.82 x 1.6 mm voxel-size, age of death=44.5  $\pm$  24.54 yrs). The cam definition step exclusively utilized the proximal femur to encompass the cam region. Five principal components were used to describe the variation in femur morphology across this cohort. To ensure the absence of a cam deformity in the normal fit of the femoral head-neck junction, the anterosuperior region of the mesh was removed prior to the fitting process. The 'healthy' proximal femur and the segmentation were then aligned using rigid

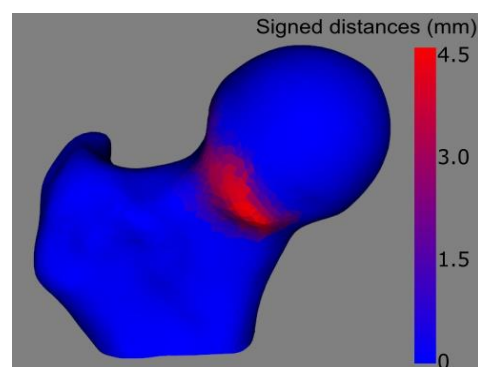


**Figure 1. Difference between healthy fit and proximal femur segmentation using signed distances at the anterosuperior region of the head neck junction.**

registration. After the alignment, signed distances between both meshes at the anterosuperior head-neck junction (typical region of Cam deformities) were calculated (see Fig. 1). Only values  $> 0$  mm were considered to calculate the mean distance deviation between both meshes. The classification of the mean distance deviation was based on the work of Bugeja, Xia, Chandra et al. (2022), who used four categories (negligible = 0-1.3mm, mild = 1.3-1.7mm, moderate = 1.7-2.2mm & severe =  $>2.2$ mm) based on the volumetric differences of a focused SSM to the real shape which the group then correlated to the average distance ( $p < 0.001$ ,  $r = 0.89$ ). The femur geometry was defined using the neck-shaft angle (NSA), the femoral anteversion (FNA), the neck length and the femoral length. Measurements were made using a custom python script to ensure repeatability (see Table 1).

**Table 1: Description of parameter calculation for the femoral geometry.**

<i>Neck shaft angle</i>	<ol style="list-style-type: none"> <li>1. Find the femur neck centre (NC) by locating its point-cloud centroid.</li> <li>2. Calculate centroids for proximal and distal shaft point-clouds.</li> <li>3. Determine the closest point to NC on a plane (CPNC) perpendicular to the femur centre, proximal shaft, and distal shaft.</li> <li>4. Calculate the angle between the neck shaft line (from femur centre to CPNC) and the diaphyseal shaft line (connecting proximal and distal shaft centroids).</li> </ol>
<i>Femoral anteversion</i>	<ol style="list-style-type: none"> <li>1. Define the centre of the medial and lateral epicondyle using ellipsoidal fits.</li> <li>2. Project the neck-shaft line and the line between the ellipsoidal fit centres onto the transverse plane and calculate the resulting angle.</li> </ol>
<i>Neck length</i>	<ol style="list-style-type: none"> <li>1. Define the minimum distance between the neck-shaft line and the diaphyseal line, expected to be zero since both lines are on the same plane.</li> <li>2. Calculate the distance between the femur centre and the point of closest distance.</li> </ol>
<i>Femur length</i>	<ol style="list-style-type: none"> <li>1. Define the femoral notch centre by finding the midpoint of ellipsoidal fits and setting the y-coordinate to the lowest y-value in the point-cloud.</li> <li>2. Calculate the distance between the femur centre and the point determined in the previous step.</li> </ol>

Statistical analysis was conducted using the statsmodel library in Python. Assumptions for Multivariate Analysis of Variance (MANOVA) were checked. If the result demonstrated significance ( $\alpha < 0.05$ ), univariate analysis of variance (ANOVA) with adapted  $\alpha$ -value ( $\alpha_{uni} = \frac{\alpha}{IV}$ , IV = number independent variables) to avoid a type 1 error was conducted, followed by Tukey's HSD test for pairwise comparison ( $\alpha < 0.05$ ).

**RESULTS:** A total of 382 full femur segmentations were analysed. 3D classification revealed 237 femora in class negligible, 80 in mild, 47 in moderate and 17 in severe (see Tab. 2). The MANOVA revealed a significant effect (Wilks' Lambda = 0.91,  $F = 2.90$ ,  $p < 0.05$ ). Follow up univariate ANOVA showed a significant effect between NSA and cam classification ( $F = 7.53$ ,  $p < 0.0125$ ). Pairwise comparison by Tukey's HSD test revealed a significant effect of NSA between negligible/moderate, negligible/severe and mild/severe ( $p < 0.01$ ) (see Fig.2) with a percentage decrease from negligible to severe of 4%. No significant difference between groups for FNA, femur length or neck length were found.

**Table 2: Descriptive results of cam categorization and femoral parameters.**

Parameter	Negligible	Mild	Moderate	Severe
n (total of 382) (%)	237 (62%)	80 (21%)	47 (12%)	17 (4%)
NSA (°)	128.1 $\pm$ 5.3	127.7 $\pm$ 5.5	125.4 $\pm$ 5.4	123.0 $\pm$ 4.9
FNA (°)	14.7 $\pm$ 8.7	13.4 $\pm$ 9.2	15.7 $\pm$ 8.1	15.1 $\pm$ 7.3
Femur Length (mm)	441.6 $\pm$ 24.1	442.8 $\pm$ 25.3	440.8 $\pm$ 24.9	447.9 $\pm$ 29.7
Neck Length (mm)	51.7 $\pm$ 5.1	51.5 $\pm$ 5.0	50.6 $\pm$ 6.8	52.6 $\pm$ 7.2

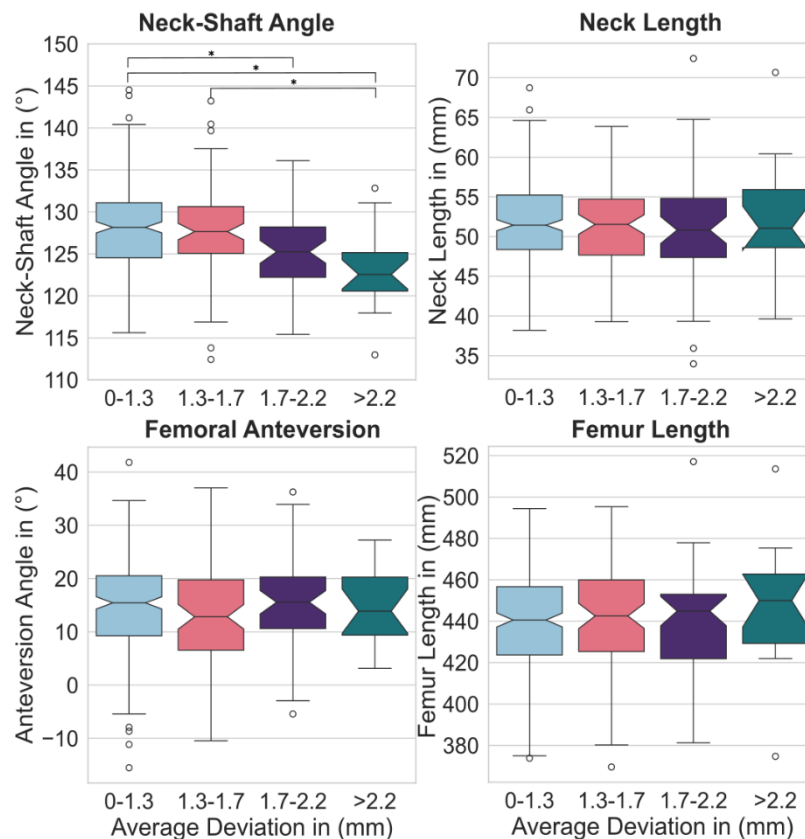


**Figure 2. Variation in femur geometry relative to cam deviation. Note significant differences only in the neck-shaft angle between groups identified as Negligible (0-1.3), Moderate (1.7-2.2) and Severe deviation (>2.2).**

**DISCUSSION:** NSA demonstrated a significant effect on the size of the cam deformity. Agricola et al. (2013) found similar results for the age group 12-15 years, nevertheless, cam categorization was based on the alpha angle and the NSA was defined on a planar radiograph with only the proximal femur in the field of view. Decreasing NSA effects the resultant reaction force applied on the acetabulum. The force decreases and shifts it medially and hence decreases the articular compressive stresses since the force is applied to a larger than normal weight bearing area (Maquet, 1985). Geoffrey et al., (2019) showed in their finite element study that with a decreasing NSA a higher stress at the anterosuperior region of the head neck junction is experienced, coinciding with the common location of a cam deformity. Additionally, the moment arms of the hip extension muscles are influenced by a decreasing neck-shaft angle, which might affect hip stability during movement due to increasing muscle forces needed by the extensor muscles (Kainz, Mindler, & Kranzl, 2023). These findings are supported by the study of Diamond et al. (2016), who showed that hip extensors of subjects with FAIS were 23% weaker than healthy controls. The lack of adequate hip abductor strength affects pelvis control and might lead towards an impinging position of the hip during movement (Diamond, et al., 2018).

FNA, femur length and neck length did not exhibit a significant effect. Schaver et al. (2021) analysed the relation between cam morphology and FNA and found a difference in FNA depending on cam morphology. This may be attributed to their method of capturing axial photos of the femur and measuring both parameters from a single projected image. Our study used ellipsoidal fit to the condyles to define the knee joint centre line as well as sphere fitting for the femur head centre and centroid calculation of the femoral neck to calculate the femoral anteversion, which might account for discrepancies in the effect.

The prevalence seen in this study of cam deformation in a general population with a rough distribution of every third male showing a deformation is in accordance with current literature (Laborie, et al., 2011). Bugeja, Xia, Candra et al. (2023) first evaluated and categorized the

cam morphology based on a three-dimensional volumetric measurement. However, they only analysed the cam morphology of the proximal femur. The analysis of the femoral geometry based on the distinction into four groups based on the average surface distance is a novel contribution considering the 3-dimensional geometry of a cam deformation. The automation based on a standardized cam location and python pipeline also assures reliability of the method for future clinical application. Our method addresses the often-criticised alpha angle which shows moderate to poor inter- and intra- reader reliability (Dessouky , et al., 2019)

**CONCLUSION:** This study identified a decreased NSA as potential risk factor for the development of a cam morphology using a novel, repeatable, 3D assessment tool to characterise cam deformities and femur geometry. Athletes with known decreased NSA but also athletes during adolescent with unknown NSA, engaging in repetitive loading situation must include hip abductor strengthening into their schedule to compensate the unfavourable lever arm.

## REFERENCES

- Agricola, R., Waarsing, J., Thomas, G., Carr, A., Reijman, M., Bierma-Zeinstra, S. & Arden, N. (2014). Cam impingement: defining the presence of a cam deformity by the alpha angle: data from the CHECK cohort and Chingford cohort. *Osteoarthritis Cartilage*, 218-25.
- Agricola, R., Heijboer, M., Ginai, A., Roels, P., Zadpoor, A., Verhaar, J. & Waarsing, J. (2014). A Cam Deformity Is Gradually Acquired During Skeletal Maturation in Adolescent and Young Male Soccer Players. *The American Journal of Sports Medicine*, 798-806.
- Bizzini, M., Schaub, G., Ferrari, E., Monn, S., Leunig, M., Casartelli, N., & Maffiuletti, N. (2023). Hip muscle strength in male and female patients with femoroacetabular impingement syndrome: Comparison to healthy controls and athletes. *Phys Ther Sport*, 142-146.
- Dessouky , R., Chhabra, A., Zhang, L., Gleason, A., Chopra, R., Chatzinoff, Y. & Wells, J. (2019). Cam-type femoroacetabular impingement-correlations between alpha angle versus volumetric measurements and surgical findings. *Eur Radiol*, 3431-40.
- Diamond, L., Bennell, K., Wrigley, T., Hinman, R., Hall, M., O'Donnell, J., & Hodges, P. (2018). Trunk, pelvis, and hip biomechanics in individuals with femoroacetabular impingement syndrome: Strategies for step ascent. *Gait & Posture*, 176-182.
- Geoffrey, K., Mantovani, G., Lamontagne, M., Labrosse, M., & Beaulé, P. (2019). Cam FAI and Smaller Neck Angles Increase Subchondral Bone Stresses During Squatting: A Finite Element Analysis. *Clinical Orthopaedics and Related Research*, 1053-1063.
- Ito, K., Minka, M., Leuning, M., Werlen, S., & Ganz, R. (2001). Femoroacetabular impingement and the cam-effect. A MRI-based quantitative anatomical study of the femoral head-neck offset. *J Bone Joint Surg Br.*, 171-176.
- Kainz, H., Mindler, G., & Kranzl, A. (2023). Influence of femoral anteversion angle and neck-shaft angle on muscle forces and joint loading during walking. *PLoS ONE*.
- Laborie, L., Lehmann, T., Engesaeter, I., Eastwood, D., Engesaeter, L., & Rosendahl, K. (2011). Prevalence of Radiographic Findings Thought to Be Associated with Femoroacetabular Impingement in a Population-based Cohort of 2081 Healthy Young Adults. *Journal of Radiology*, 494-502.
- Maquet, P. (1985). *Biomechanics of the Hip*. Berlin: Springer-Verlag.
- Palmer, A., Scott, F., Gimpel, M., Birchall, R., Judge, A., Broomfield, J. & Glyn-Jones, S. (2018). Physical activity during adolescence and the development of cam morphology: a cross-sectional cohort study of 210 individuals. *J Sports Med*, 601-610.
- Schaver, A., Oshodi, A., Glass, N., Duchmann, K., Willey, M., & Westermann, R. (2021). Cam Morphology Is Associated with Increased Femoral Version: Findings from a Collection of 1321 Cadaveric Femurs. *Arthroscopy: The Journal of Arthroscopic and Related Surgery*, 1-6.

**ACKNOWLEDGEMENTS:** This publication was made possible with the support of the International Society of Biomechanics Travel Grant, the Doctorate Grant from the German Academic Exchange Service. We also acknowledge the Victorian Institute of Forensic Medicine (VIFM) for providing the CT images, which were segmented for this study.